Zhu et al. Journal of Cardiovascular Magnetic Resonance (2019) 21:72
https://doi.org/10.1186/s12968-019-0583-y

Journal of Cardiovascular Magnetic Resonance

TECHNICAL NOTES Open Access

T_2STIR preparation for single-shot cardiovascular magnetic resonance myocardial edema imaging

Yanjie Zhu[1], Dan Yang[2], Lixian Zou[1], Yucheng Chen[2], Xin Liu[1] and Yiu-Cho Chung[3*]

Abstract

Background: Myocardial edema in acute myocardial infarction (AMI) is commonly imaged using dark-blood short tau inversion recovery turbo spin echo (STIR-TSE) cardiovascular magnetic resonance (CMR). The technique is sensitive to cardiac motion and coil sensitivity variation, leading to myocardial signal nonuniformity and impeding reliable depiction of edematous tissues. T_2-prepared balanced steady state free precession (T_2p-bSSFP) imaging has been proposed, but its contrast is low, and averaging is commonly needed. T_2 mapping is useful but requires a long scan time and breathholding. We propose here a single-shot magnetization prepared sequence that increases the contrast between edema and normal myocardium and apply it to myocardial edema imaging.

Methods: A magnetization preparation module (T_2STIR) is designed to exploit the simultaneous elevation of T_1 and T_2 in edema to improve the depiction of edematous myocardium. The module tips magnetization down to the –z axis after T_2 preparation. Transverse magnetization is sampled at the fat null point using bSSFP readout and allows for single-shot myocardial edema imaging. The sequence (T_2STIR-bSSFP) was studied for its contrast behavior using simulation and phantoms. It was then evaluated on 7 healthy subjects and 7 AMI patients by comparing it to T_2p-bSSFP and T_2 mapping using the contrast-to-noise ratio (CNR) and the contrast ratio as performance indices.

Results: In simulation and phantom studies, T_2STIR-bSSFP had improved contrast between edema and normal myocardium compared with the other two edema imaging techniques. In patients, the CNR of T_2STIR-bSSFP was higher than T_2p-bSSFP (5.9 ± 2.6 vs. 2.8 ± 2.0, $P < 0.05$) but had no significant difference compared with that of the T_2 map (T_2 map: 6.6 ± 3.3 vs. 5.9 ± 2.6, $P = 0.62$). The contrast ratio of T_2STIR-bSSFP (2.4 ± 0.8) was higher than that of the T_2 map (1.3 ± 0.1, $P < 0.01$) and T_2p-bSSFP (1.4 ± 0.5, $P < 0.05$).

Conclusion: T_2STIR-bSSFP has improved contrast between edematous and normal myocardium compared with commonly used bSSFP-based edema imaging techniques. T_2STIR-bSSFP also differentiates between fat that was robustly suppressed and fluids around the heart. The technique is useful for single-shot edema imaging in AMI patients.

Keywords: T_2STIR, Edema, Single-shot imaging, Short tau inversion recovery

* Correspondence: yiu-cho.chung@siemens.com
[3]Siemens Healthcare Pte Ltd., 60 MacPherson Road, Singapore 348615, Singapore
Full list of author information is available at the end of the article

Background

As myocardial edema has long T_2, T_2-weighted cardiovascular magnetic resonance (CMR) imaging is usually used in the imaging of acute myocardial infarction (AMI) [1–3], where edema commonly occurs. T_2-weighted turbo spin echo (TSE) combined with short tau inversion recovery (STIR) and dark-blood preparation (STIR-TSE) has been widely used clinically for this purpose [4]. However, the technique is sensitive to cardiac motion, leading to signal loss and hence myocardial signal inhomogeneity. Coil sensitivity variation increases variation of the myocardial signal. Additionally, the stagnant blood at the subendocardial rim would sometimes mimic edematous tissues. These issues of STIR-TSE impede reliable depiction of edematous tissues [5, 6]. Moreover, STIR-TSE is sensitive to arrhythmia and respiratory motion.

Several CMR techniques have been proposed to address these issues of STIR-TSE for myocardial edema imaging. The STIR pulse in STIR-TSE is sometimes replaced by the spectral attenuated inversion recovery (SPAIR) pulse for fat suppression [7] to reduce motion sensitivity. The method is sensitive to main field inhomogeneity. It has also been shown that the technique depends on the proper choice of image readout time [6]. Single-shot T_2-prepared balanced steady state free precession (T_2p-bSSFP) [8] shows higher diagnostic accuracy than STIR-TSE for edema imaging [9, 10]. It is robust to cardiac motion and arrhythmia and avoids the bright subendocardial rims caused by stagnant blood that mimic myocardial edema as in STIR-TSE. However, it is sensitive to coil sensitivity variation, and multiple acquisitions are commonly needed to improve image SNR. Another method, ACUT$_2$E [11], improves T_2 weighting intrinsic in bSSFP by using 180° excitation pulses. Yet, high flip angles for the excitation pulses might not be achieved due to the specific absorption rate (SAR) limit and the technique's sensitivity to transmit (B_1+) field inhomogeneity, especially at a high field. Similar to STIR-TSE, ACUT$_2$E is a segmented sequence and is sensitive to arrhythmia and respiratory motion as well.

T_2 mapping [12–15] CMR was proposed for myocardial edema imaging [16]. T_2 quantification can help objectively distinguish between normal and edematous myocardium. It can also detect myocarditis with systematic T_2 elevation in myocardium. In this method, several T_2p-bSSFP images with different echo times are acquired over multiple heart beats. The T_2 map is then obtained through pixelwise curve fitting of these T_2-weighted images upon image registration. The technique is sensitive to arrhythmia and requires breathholding. Moreover, the accuracy of T_2 maps depends on multiple factors, e.g., heart rate, fitting model, the patient's breathholding ability, off-resonance effect, etc. [13, 17–19].

Recent parametric mapping studies on myocardial edema reaffirmed earlier findings [20] that both T_1 and T_2 values are increased in edematous tissues [21, 22]. Although the native T_1 of myocardium also increases in the presence of fibrosis, there is no measurable fibrosis expected at 2 to 5 days post-reperfusion. Therefore, any increase in myocardial T_1 most likely comes from edema. Thus, a CMR sequence that exploits the elevation of both T_1 and T_2 values may yield an edema detection method at a higher specificity. bSSFP cine, whose signal is proportional to $\sqrt{(T_2/T_1)}$, has been proposed to depict edematous tissue [23]. However, the signal equation shows that the signal increase due to T_2 elevation is attenuated by the concomitant increase in T_1. The resulting signal change is small. The method is therefore sensitive to coil sensitivity variation. Postcontrast bSSFP cine shortens myocardial T_1 values and improves the contrast between edematous and normal myocardium [24]. The use of contrast agents increases patient risk. Also, the image contrast depends on contrast dosage and the delay time after contrast injection.

This study proposes a novel single-shot CMR technique for edema imaging. The new technique uses a magnetization preparation module called T_2STIR (T_2 prepared inversion with STIR) to exploit the simultaneous elevation of T_1 and T_2 in edematous tissues for improved differentiation of edematous and normal myocardium while suppressing fat. The module is combined with single-shot bSSFP, making it insensitive to arrhythmia and breathing motion. The performance of the resulting single-shot sequence is assessed by simulation, a phantom study, and in vivo studies in healthy subjects. The technique is finally applied to a small number of patients with known myocardial edema to demonstrate its clinical feasibility. The preliminary work of this study was first reported in [25].

Theory

The T_2STIR preparation module

Figure 1 (a) shows the signal evolutions of edema and normal myocardium with the T_2STIR module. Contrast of the T_2STIR module between edema and normal myocardium is generated by T_2 preparation together with spin inversion. Upon inversion of the T_2 prepared magnetization, the longitudinal magnetization of a tissue is given by:

$$M_z = -M_0 \cdot e^{-TE_{prep}/T_2} \quad (1)$$

Here, TE_{prep} is the echo time of the T_2 preparation module, and T_2 is the spin-spin relaxation time of the

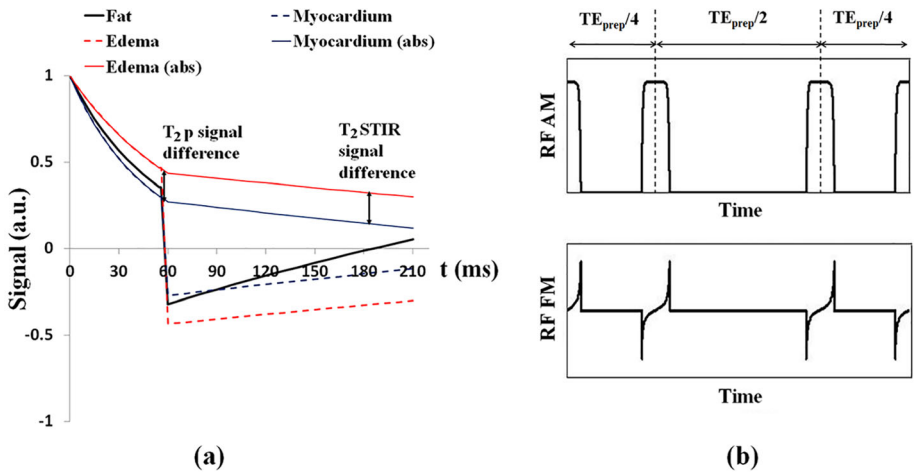

Fig. 1 **a** The difference between a T_2 preparation module and the T_2 short tau inversion recovery (STIR) module in preparing the magnetization of the myocardial tissues for imaging. The T_2STIR module tips the magnetization down to the –z axis after T_2 preparation. **b** The amplitude and frequency modulation of the adiabatic T_2STIR magnetization preparation module

tissue. The resulting magnetization is then sampled at TI_{fat}, the fat null point, which is given by:

$$TI_{fat} = T_{1,fat} \cdot \ln\left(1 + e^{-TE_{prep}/T_{2,fat}}\right) \quad (2)$$

where $T_{1,\ fat}$ and $T_{2,\ fat}$ are the T_1 and T_2 relaxation times for fat.

After spin inversion, normal myocardium recovers faster than edematous myocardium (see Fig. 1(a)). With magnitude reconstruction, inverted magnetization is "reverted": edematous tissues now have higher signal intensity than normal myocardium. The inversion and the partial recovery over TI accentuate the signal difference between edema and normal myocardium generated by T_2 preparation alone. Here, the choice of TI to null fat is similar to the STIR pulse. This new magnetization preparation module is hereby referred to as T_2STIR.

Equation (2) shows that TI_{fat} is determined by T_1 and T_2 of fat (which are 449 ms and 53 ms at 3 T, respectively [26]) and the TE_{prep} used in the T_2 preparation part of the pulse. For instance, at TE_{prep} = 60 ms, TI_{fat} would be 125 ms.

T_2STIR-prepared single-shot edema imaging

Figure 1(b) shows the implementation of the T_2STIR module designed based on the modified B_1-insensitive rotation pulse (mBIR-4) [27]. It has three components: a reverse adiabatic half passage (rAHP) pulse, followed by an adiabatic full passage (AFP) pulse and finally an adiabatic half passage (AHP) pulse. The AFP pulse is used twice to reduce the module's sensitivity to B_0 and B_1+ field inhomogeneity [28]. The phase shift and delay times among the four pulses are designed to flip the transverse magnetization down to the $-M_z$ direction after T_2 preparation. The rAHP pulse, AFP pulse and AHP pulse are 2.56 ms, 5.12 ms and 2.56 ms long, respectively, giving a minimum TE_{prep} of 15.36 ms. The frequency sweep is 4.88 kHz. A spoiler gradient at the end of the module destroys any coherent transverse magnetization after the preparation module. Figure 1(b) shows the amplitude and frequency modulations of this adiabatic T_2STIR preparation pulse based on the tan/tanh modulation function.

Imaging is performed using the single-shot bSSFP readout, similar to that of T_2p-bSSFP. Linear flip angle (LFA) pulses for catalysis [29] and linear reordering are used to minimize transient oscillations in bSSFP at the start of acquisition [12]. The acquisition is timed to mid-diastole. The sequence is hereafter referred to as T_2STIR-bSSFP.

In T_2STIR-bSSFP, TI_{fat} is the time from the end of the T_2STIR module to the k-space center of the bSSFP readout. Let TI_{fill} be the fill time between the end of the T_2STIR module and the start of bSSFP readout. Then,

$$TI_{fill} = TI_{fat} - (R + N) \cdot TR \quad (3)$$

where R is the number of LFA pulses, and N is the number of lines acquired between the end of the LFA pulse train and the k-space centerline. As $TI_{fill} \geq 0$, the choice of R and N together set the lower limit of TI_{fat}, and hence the maximum TE_{prep} allowed. Experience from T_2p-bSSFP shows that a TE_{prep} of 60 ms is commonly used to generate T_2-induced signal differences for the differentiation of edema and normal myocardium [8]. If this same TE_{prep} is used in the T_2STIR module, it corresponds to a TI_{fat} of approximately 125 ms and would satisfy Eq. (3).

Methods

Simulation

T_2STIR-bSSFP was compared with T_2p-bSSFP with TE_{prep} varying from 40 ms to 70 ms through Bloch equation simulation using MATLAB (version 2017a, The MathWorks Inc., Natick, Massachusetts, USA). The parameters for bSSFP readout used in the simulation were as follows: 10 LFA pulses, 22 phase encoding lines before the k-space center, flip angle = 60°, TE/TR = 1.3/2.6 ms. The T_1 and T_2 values were 1139 ms and 52 ms for normal myocardium and 1434 ms and 75 ms for edematous tissue. They were the relaxation parameters of the compartments in the phantom study below.

Phantom study

A phantom experiment was performed to evaluate the performance of T_2STIR-bSSFP and compare it with T_2p-bSSFP and T_2 mapping [12]. The sequence was implemented on a 3 T clinical CMR system (TIM TRIO, Siemens Healthineers, Erlangen, Germany) for all experiments. A two-compartment phantom, one for normal myocardium and the other for edema, was built with agar doped with $NiCl_2$. The T_1 values of the compartments were measured using an inversion recovery spin echo sequence (TR = 10 s, TI changing from 100 ms to 3600 ms). The T_2 values were measured using a spin echo sequence (TR = 10 s, TE varying from 10 ms to 150 ms). The T_1 and T_2 values were 1139 ms and 52 ms for normal myocardium compartment and 1434 ms and 75 ms for edema compartment, respectively.

The phantom was imaged with T_2STIR-bSSFP, T_2p-bSSFP, and T_2 mapping [12]. Simulated electrocardiogram (ECG) with an RR interval of 800 ms was used. The value of TE_{prep} in the T_2STIR and T_2p modules was varied from 40 ms to 70 ms in 5 ms increments. Imaging parameters identical to all sequences were as follows: FOV = 240 × 83 mm^2, matrix size = 128 × 44, pixel size = 1.9 × 1.9 mm^2, slice thickness = 8 mm, TE/TR = 1.3/2.6 ms, bandwidth = 1447 Hz/pixel, flip angle = 60°. Parallel imaging was not used, allowing accurate estimation of signal and noise in the images. The experiments were repeated four times. Images were then averaged for analysis.

Healthy subject study

A protocol for in vivo imaging was developed and evaluated in healthy subjects. Blood was used as a surrogate for edema because its T_1 and T_2 values were both longer than normal myocardium. The study was approved by the institutional review board (IRB) at Shenzhen Institutes of Advanced Technology. Seven healthy subjects (5 males, 26 ± 3 years) were recruited, and informed consent was obtained. For each subject, three short axis slices (basal, mid-ventricular and apical) and one horizontal long axis of the heart were acquired using T_2STIR-bSSFP and T_2p-bSSFP. Imaging parameters for both single-shot sequences were identical: FOV = 360 × 260 mm^2, matrix size = 192 × 138, pixel size = 1.9 × 1.9 mm^2, slice thickness = 8 mm, TE/TR = 1.3/2.6 ms, flip angle = 60°, bandwidth = 1447 Hz/pixel, phase resolution = 75%, TE_{prep} = 60 ms, and TI_{fill} was 20 ms (TI_{fat} = 125 ms) in T_2STIR-bSSFP. GRAPPA rate 2 with 24 auto-calibration lines was used to reduce the image acquisition window.

Patient study

The ability of the three imaging techniques (T_2STIR-bSSFP, T_2p-bSSFP and T_2 mapping) in detecting edema was evaluated in AMI patients. The study was approved by the IRB of West China Hospital, where patient recruitment and scanning were carried out. Seven patients (5 males, 60 ± 10 years) with ST-segment elevation myocardial infarction (STEMI), identified by clinical presentation, ECG and coronary angiograms, were recruited after reperfusion. Informed consent was obtained from each patient. The patients were examined on days 2 to 5 post-reperfusion using the institution's standard CMR protocols, including STIR-TSE, T_1 maps [30] and T_2 maps [12] on a 3 T CMR scanner (TIM TRIO, Siemens Healthineers). The patients were then imaged with T_2STIR-bSSFP and T_2p-bSSFP (using the protocols in the healthy subject study). Late gadolinium enhancement (LGE) images were then acquired for each patient approximately 10 min after the injection of gadolinium-based contrast agent (0.15 mmol/kg, Magnevist, Bayer, Whippany, New Jersey, USA). Imaging parameters of the relevant sequences are listed in Table 1.

Data analysis

The performance of T_2STIR-bSSFP was assessed by (1) the signal difference in the simulation or the contrast-to-noise ratio (CNR) in images and (2) the contrast ratio between edema and normal myocardium [20]. In the images, signal intensity (SI) was given by the mean signal of the region of interest (ROI). Noise was given by the standard deviation (SD) of normal myocardium [31]. The equations to find the signal difference, signal to noise ratio (SNR), CNR, and contrast ratio for T_2p-bSSFP and T_2STIR-bSSFP, as well as the calculation of SNR, CNR and contrast ratio for the T_2 maps, are defined in the Additional file 1.

In the phantom study, ROIs were manually drawn for each compartment. The signal difference and the contrast ratio between the normal and edematous myocardium compartments of the phantom for T_2STIR-bSSFP and T_2p-bSSFP at each TE_{prep} were found. The correlation between the simulation and the phantom study was assessed by linear regression. The contrast ratio of the T_2 value between the normal and edematous

Table 1 Imaging parameters used in the patient study

	T_1 mapping	T_2 mapping	T_2p/T_2STIR-bSSFP	STIR-TSE[a]	LGE
TE/TR	1.15/2.7 ms	1.09/2.5 ms	1.3/2.6 ms	62/2 RR	3.4/6.6 ms
Image matrix	256 × 216	192 × 160	192 × 144	256 × 216	256 × 216
Resolution	1.4 × 1.9 mm	1.9 × 2.5 mm	1.9 × 2.5 mm	1.4 × 1.4 mm	1.4 × 1.4 mm
Readout	bSSFP	bSSFP	bSSFP	TSE	GRE
Flip angle	35°	35 °	60 °	90°	20°
Bandwidth (Hz/pixel)	1085	1447	1447	781	287
Echo train	n.a.[b]	n.a.	n.a.	15	n.a.
TE_{prep}	n.a.	0, 25, 55 ms	60 ms	n.a.	n.a.
Scan time (heartbeats)	11	7	1	12	8
Acquisition	"Single-shot", multiple acq.		Single-shot	Segmented	Segmented
Parallel imaging	GRAPPA rate 2				

[a]The STIR-TSE sequence was not included in the sequence performance comparison LGE, late gadolinium enhancement TE, echo time TR, repetition time
[b] n.a. means "not applicable"

myocardium compartments in the T_2 map was also calculated.

For healthy subjects, the ROIs of myocardium and blood pool were manually drawn for each subject. The myocardial signal was measured at the septum. Blood signals were measured at the center of the blood pool in the left ventricle. The CNRs and contrast ratios between the myocardium and the blood (surrogate for edema) of T_2STIR-bSSFP and T_2p-bSSFP were calculated for each slice. The average CNRs and contrast ratios over all the slices were recorded for each sequence.

For AMI patients, the ROI of remote myocardium was manually drawn on the LGE images by an experienced reader (5-year CMR experience). This ROI was copied and pasted on T_1 map and T_2 map to keep the ROI position the same as on the LGE image. The ROIs on T_1 and T_2 maps were slightly adjusted to ensure the entire ROI was inside the myocardium if the myocardium on T_1 or T_2 map was not aligned with the myocardium on LGE image due to motion. The mean and SD values of these regions were calculated for the T_1 and T_2 maps. Myocardial regions with T_1 and T_2 values larger than the mean + 2 SD of the remote myocardium were identified as edematous regions. At the regions where both T_1 and T_2 were elevated (the two parametric maps may have slightly different shapes), contours for signal measurement were manually drawn inside these regions. Regions of microvascular obstructions (identified on LGE images) and artifacts (i.e., motion artifact, banding artifact), if present, were excluded from the ROIs. The CNR and contrast ratio between the myocardium and edema in each image were calculated for T_2STIR-bSSFP, T_2p-bSSFP, and T_2 mapping. The two performance indices were then averaged among the patients for each imaging method compared in this study. The CNR and contrast ratio differences (given as the mean ± SD) among the three sequences compared were tested for statistical significance. The data were tested for a normal distribution using the Kolmogorov-Smirnov Test. The CNR and the contrast ratio among the different methods were compared using the Mann-Whitney U-test. Statistical significance was set at $P < 0.05$. The extents of edema determined by the different methods are shown in Additional file 1. Note that the STIR-TSE was not included in the sequence comparison in this study since previous clinical studies already showed that T_2p-bSSFP has better diagnostic accuracy than STIR-TSE [8, 10].

Results

Simulation

The variation in signal difference and contrast ratio between normal myocardium and edema with TE_{prep} in T_2STIR-bSSFP and T_2p-bSSFP are shown in Fig. 2. The contrast ratio of the T_2 values between the two compartments is also shown in Fig. 2(b) for comparison. The signal differences in T_2STIR-bSSFP are higher than those of T_2p-bSSFP and are insensitive to TE_{prep} in both cases. Meanwhile, the contrast ratios of the two sequences increase with TE_{prep}. The contrast ratio increases faster with TE_{prep} for T_2STIR-bSSFP than for T_2p-bSSFP. T_2STIR-bSSFP has the highest contrast ratio among the three edema imaging sequences compared. Note that the contrast ratios from T_2p-bSSFP and the T_2 map are similar, as both were T_2 prepared in the same way.

At TE_{prep} = 60 ms, the signal difference between edema and normal myocardium in T_2STIR-bSSFP is 15% higher than that of T_2p-bSSFP. At the same TE_{prep}, the contrast ratios between edema and normal myocardium for T_2p-bSSFP and T_2 map are approximately the same and are approximately 30% lower than that of T_2STIR-bSSFP.

Phantom study

The signal differences of the simulation and the phantom study showed strong correlations for T_2p-bSSFP

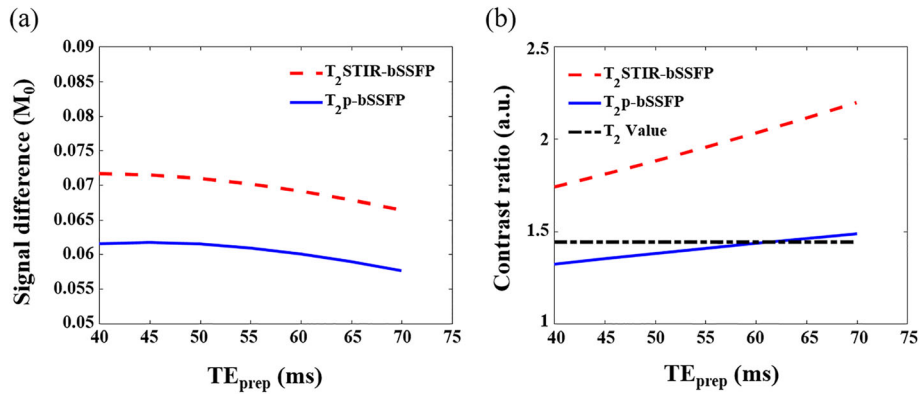

Fig. 2 The change in (**a**) signal differences and (**b**) contrast ratios between edematous and normal myocardium with TE_{prep} in T_2STIR-balanced steady state free precession (bSSFP) and T_2p-bSSFP in simulation. The signal differences are defined in normalized units of equilibrium magnetization (M_0). The contrast ratio of T_2 value between edematous and normal myocardium is also shown for comparison. T_2STIR-bSSFP has a higher signal difference than T_2p-bSSFP and has the highest contrast ratio among the three edema imaging sequences. The contrast ratios from T_2p-bSSFP and the T_2 map are similar, as both were T_2-prepared in the same way. The contrast ratio of T_2STIR-bSSFP increases faster with TE_{prep} than that of T_2p-bSSFP

($R^2 = 0.90$) and T_2STIR-bSSFP ($R^2 = 0.89$) (Fig. 3(a)). Excellent correlations between the contrast ratios of the simulation and the phantom study were obtained for T_2p-bSSFP ($R^2 = 0.99$, slop = 0.99) and T_2STIR-bSSFP ($R^2 = 0.98$, slop = 0.98) (Fig. 3(b)). The T_2 values measured by T_2 mapping were 74 ms and 55 ms for the two phantom compartments representing edema and normal myocardium, respectively. The corresponding contrast ratio for the T_2 map (1.36) is very close to the expected value (1.44).

In vivo experiments

Healthy subject study

The average CNR between myocardium and blood (surrogate for edema) of T_2STIR-bSSFP was higher than that for T_2p-bSSFP (29.6 ± 8.3 vs. 19.0 ± 5.7, $P < 0.001$). The average contrast ratio of T_2STIR-bSSFP was also higher than that of T_2p-bSSFP (6.1 ± 0.9 vs. 2.9 ± 0.5, $P < 0.001$).

Patient study

Among the seven AMI patients, four had microvascular obstruction. They were identified and excluded from the corresponding ROIs. Table 2 summarizes the mean and SD of SI and SNR for normal and edematous myocardium for all the edema imaging techniques compared. Among the three methods, T_2 map has the smallest coefficient of variation (which is the reciprocal of SNR). Figure 4 shows the CNRs and the contrast ratios of T_2 map, T_2p-bSSFP, and T_2STIR-bSSFP in bar graphs. The CNR of T_2STIR-bSSFP was higher than that of T_2p-bSSFP (5.9 ± 2.6 vs. 2.8 ± 2.0, $P < 0.05$). There was no significant difference between the CNRs of the T_2 map and

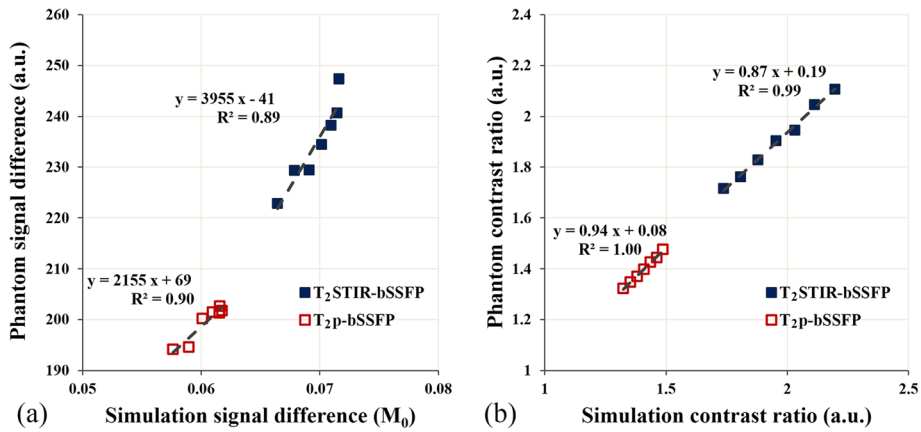

Fig. 3 **a** Correlation between the signal differences in the simulation and the phantom study for T_2p-bSSFP and T_2STIR-bSSFP. **b** Correlations between the contrast ratios of the simulation and the phantom study for T_2p-bSSFP and T_2STIR-bSSFP

Table 2 Summary of average mean and standard deviation of the signal and the signal to noise ratio (SNR) for normal and edematous myocardium

	T_1 map	T_2 map	T_2p-bSSFP	T_2STIR-bSSFP
Myocardial signal	1218 ± 76 ms	43 ± 3 ms	90 ± 11	37 ± 9
Edema	1493 ± 48 ms	57 ± 4 ms	124 ± 16	86 ± 14
SNR of normal myocardium	34.7 ± 8.2	16.3 ± 5.4	9.9 ± 4.2	5.0 ± 1.5
SNR of edema	41.7 ± 10.7	21.9 ± 8.1	12.8 ± 4.8	9.9 ± 3.1

T_2STIR-bSSFP (T_2 map: 6.6 ± 3.3 vs. 5.9 ± 2.6, $P = 0.62$). However, the contrast ratio of T_2STIR-bSSFP (2.4 ± 0.8) was higher than that of the T_2 map (1.3 ± 0.1, $P < 0.01$) and T_2p-bSSFP (1.4 ± 0.5, $P < 0.05$).

Figure 5 shows the images from one AMI patient. The infarct region in the LGE image matched the location where both T_1 and T_2 were elevated in the two parametric maps. The dark core inside the edema/infarct in LGE (where T_1 and T_2 in the parametric maps were both low) most likely corresponded to microvascular obstruction. The signal from the normal myocardium in T_2STIR-bSSFP was lower than that of T_2p-bSSFP, making the edematous region in T_2STIR-bSSFP obvious. Note the bright signal surrounding the heart (yellow arrow) in both single-shot bSSFP images. The fat-suppressed T_2STIR-bSSFP image suggested that it was likely pericardial fluid. In the T_2p-bSSFP image, both epicardial fat and pericardial fluid were bright. Edema was also depicted in STIR-TSE (Fig. 5(d)).

Figure 6 shows the images from another AMI patient. T_1 and T_2 elevation from the parametric maps (Fig. 6(c) and (f)) at the septal wall suggested the presence of edema. Enhancement in the LGE image (Fig. 6(e)) matched the position of edema in the parametric maps. Again, the signal for remote myocardium in the T_2STIR-bSSFP image was lower than that in the T_2p-bSSFP image, while the reverse was true for edema. The contrast improvement in T_2STIR-bSSFP compared with T_2p-bSSFP was obvious. The edematous region also appeared in STIR-TSE (Fig. 6(d)). However, the signal of the normal myocardium is highly non-uniform and might be affected by coil sensitivity variation. The T_2STIR-bSSFP images from the remaining 5 patients are shown in Additional file 1: Figure S2.

Discussion

This study proposes a novel magnetization preparation module, T_2STIR, for single-shot myocardial edema imaging and demonstrates its relevance to myocardial edema imaging. Compared with the T_2p module, the T_2STIR module increases the contrast between edematous tissues and normal myocardium without increasing SAR. The simulation and phantom experimental results agreed well with each other. Both showed improved contrast of T_2STIR-bSSFP compared with T_2p-bSSFP and T_2 mapping. In vivo experiments showed that T_2STIR-bSSFP outperformed the other two common edema imaging methods: in healthy subjects, the technique showed an improved CNR and contrast ratio between blood and myocardium compared with T_2p-bSSFP. In patients, T_2STIR-bSSFP had higher CNR than T_2p-

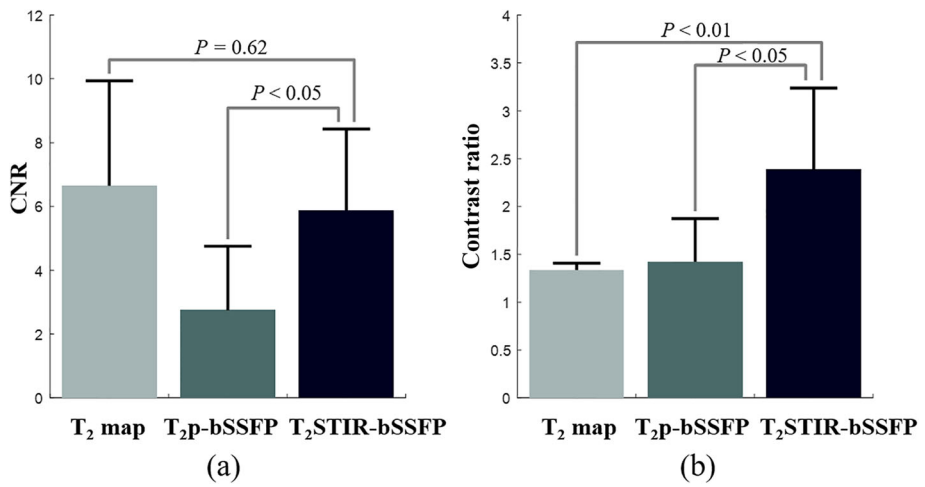

Fig. 4 Comparison of (**a**) contrast to noise ratio (CNR)s and (**b**) contrast ratios among T_2 map, T_2p-bSSFP, and T_2STIR-bSSFP. The CNR of T_2STIR-bSSFP was higher than that of T_2p-bSSFP, and the contrast ratio of T_2STIR-bSSFP was higher than that of T_2 map and T_2p-bSSFP

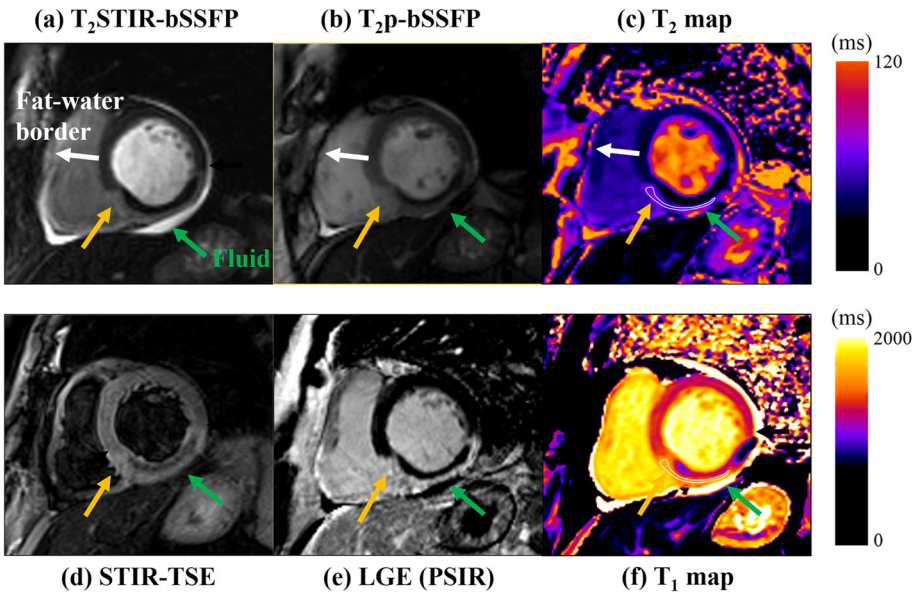

Fig. 5 Images from one AMI patient. The location of elevated T_1 and T_2 in the two parametric maps (Fig. 5(**c**) and (**f**)) corresponded to edema. The dark core inside the edema/infarct in the late gadolinium enhancement (LGE, Fig. 5(**e**)) most likely corresponded to microvascular obstruction, which had both low T_1 and T_2 in the parametric maps. The position of the dark core within the edema/infarct in LGE matched well with the STIR-TSE (Fig. 5(**d**)), T_2STIR-bSSFP (Fig. 5(**a**)) and T_2p-bSSFP (Fig. 5(**b**)) images. In the fat-suppressed T_2STIR-bSSFP image, the tissue indicated by the yellow arrow was likely pericardial fluid (yellow arrow). In the T_2p-bSSFP image, both epicardial fat and pericardial fluid were bright. The images of T_2STIR-bSSFP and T_2p-bSSFP were windowed to the same level to facilitate visual comparison

bSSFP and the highest contrast ratio compared to T_2p-bSSFP and T_2 mapping.

A T_2 preparation pulse combined with inversion recovery has been proposed in previous studies [32–36]. However, the inversion times (TI) in these applications were chosen to null tissues other than fat (normal myocardium, blood, etc.). The T_2STIR module proposed here is novel in that (1) TI is selected to suppress the tissue with the shortest T_1 (fat in this case) and (2) the inversion pulse is integrated with the T_2 preparation

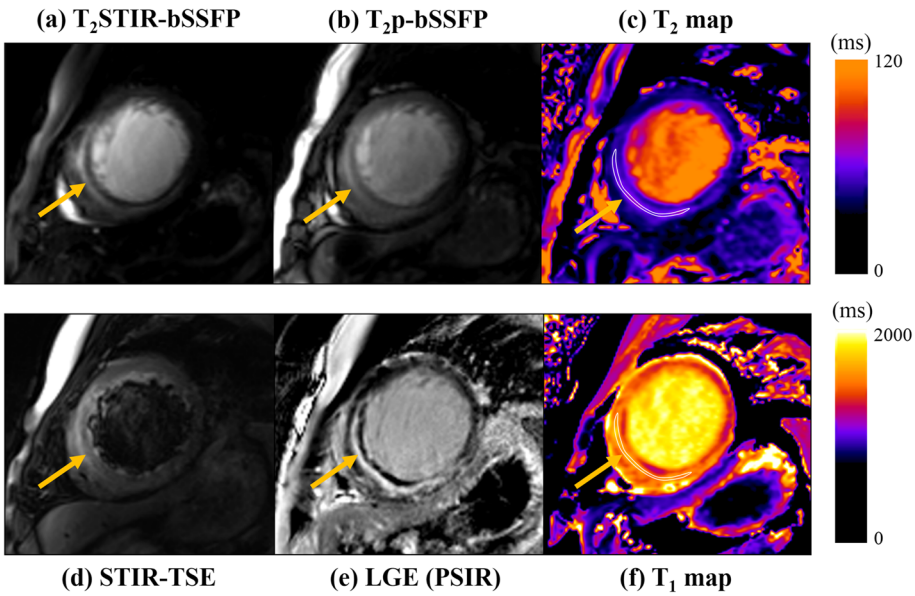

Fig. 6 Images from another AMI patient. (**a**) T_2STIR-bSSFP image (**b**) T_2p-bSSFP image (**c**) The T_2 map (**d**) The STIR-TSE image showed the edema surrounding a dark region that may correspond to microvascular obstruction. (**e**) The LGE image (**f**) The T_1 map. The images of T_2STIR-bSSFP and T_2p-bSSFP were windowed to the same level

module and reduces the SAR. Although blood is not nulled in T_2STIR-bSSFP, no flow artifact was observed in the imaging experiments, especially in the long axis view. The reason is that the T_2STIR pulse is nonselective. Additionally, image acquisition is performed in mid-diastole when blood flow is minimal. Flow artifacts are therefore much less likely.

A key feature of T_2STIR-bSSFP compared with other gradient echo-based edema imaging sequences is its robust fat suppression. It removes the dark rim at the fat-water interface and improves tissue visualization (Fig. 5(a)). Fat suppression in T_2STIR-bSSFP also helps differentiate pericardial fluid (common in AMI patients) from epicardial fat, both bright in bSSFP images (Fig. 5(b)). While fat suppression is possible with spectrally selective pulses in T_2p-bSSFP, the technique is sensitive to main field inhomogeneity and increases SAR, especially at a high field. Theoretically, the performance of fat suppression in T_2STIR-bSSFP would be affected by the T_1 and T_2 values of fat according to Eq. [2]. Incomplete inversion and the excitation pulses from the bSSFP readout before the k-space center would also affect fat suppression. Our experience with the single-shot T_2STIR-bSSFP from the in vivo imaging experiments using $TE_{prep} = 60$ ms revealed that a TI_{fat} ranging from 110 ms to 130 ms can effectively suppress fat. The choice of TI_{fat} is therefore quite forgiving in practice.

The proposed T_2STIR magnetization preparation module would be attractive at a main magnetic field beyond 3 T for two reasons. First, the T_2STIR module will have improved contrast. As T_1 increases with the magnetic field, the T_1 difference between edematous and normal myocardium is increased. The contrast between the two tissues would therefore increase at a higher magnetic field with the T_2STIR module. Additionally, the longer T_1 of fat at higher field strength allows the use of longer TE_{prep} (while TI_{fat} satisfies Eq. [2]), further improving the edema contrast of this technique. Second, T_2STIR-bSSFP is generally more favorable to other multishot edema imaging techniques in terms of SAR. For instance, single-shot T_2STIR imaging is only 33% that of T_2 mapping. However, the bSSFP readout is prone to banding artifact caused by field inhomogeneity, especially at 3 T and beyond. The banding artifact may be avoided or moved out of the ROI by using local shimming and frequency scout [37]. Alternatively, spoiled gradient readout can be used instead of bSSFP readout in single-shot T_2STIR imaging if banding artifacts still persists.

While T_2STIR-bSSFP shows the highest contrast ratio among the three edema imaging sequences compared and holds great promise for edema imaging in STEMI patients, it is not meant to replace T_2 mapping. The latter method can identify global changes in T_2 values, such as diffuse myocarditis and Takotsubo cardiomyopathy [38], for which T_2STIR-bSSFP is not applicable. In fact, the two techniques may be used together: the single-shot T_2STIR-bSSFP technique can identify edematous regions of the whole heart without requiring breath-holding. The T_2 mapping technique can then be performed at the selected location where edema is found. Taking into account the time needed for full T_1 recovery between consecutive slices, T_2STIR-bSSFP can cover the whole heart (8 slices) in approximately 40 s with no need for breath-hold.

STIR-TSE images are susceptible to coil sensitivity variation. The same is true for T_2p-bSSFP, in which the SI of edema in the images is only 25–50% [8] higher than that of normal myocardium. In T_2STIR-bSSFP, the SI of edema is 60–220% higher than of normal myocardium in both phantom and patients without coil sensitivity correction. Coil sensitivity correction is therefore optional, although it helps to further improve image contrast. In T_2 mapping, curve fitting removes the effect of coil sensitivity on T_2 values, but respiratory motion or imperfect breath-holding may increase the variability of T_2 values. Also, the estimated T_2 value in T_2 mapping may vary with arrhythmia, especially for long T_1 tissues (Additional file 1: Table S1).

In this study, the performance of three bSSFP-based sequences was evaluated using the CNR and the contrast ratio. SNR measurement in magnitude images is not accurate due to a few reasons. The use of phased array coils results in spatially non-uniform signals in magnitude images but does not affect the parametric maps. In vivo noise measurement is not easy either. The use of parallel imaging results in spatially varying noise and makes noise measurement nontrivial [39]. Image noise also depends on imaging parameters such as voxel size and readout bandwidth. In this study, noise was measured as the SD of normal myocardium [31] and was applied to both qualitative images and parametric maps. Because it is difficult to accurately measure SNR in vivo, the contrast ratio is used to complement the CNR in quantifying image contrast. The contrast ratio is independent of noise and imaging parameters used. This metric has been shown elsewhere [40, 41] to be a better indicator than CNR in describing the ability of an imaging technique to differentiate two types of tissues. Additionally, the metric is applicable to both qualitative images and parametric maps.

In addition to the SNR measurement method, the study has other limitations. Though T_2STIR-bSSFP images show edema and its positions correctly in all patient cases, its use for quantifying the extent of edema may need further study. Additional file 1 show that when the mean + 2SD was used empirically as the criterion for edema area quantification, errors exist in some cases.

While the new technique has better image contrast than other bSSFP techniques compared, the spatial variation of coil sensitivity over the T_2STIR-bSSFP images may affect accurate delineation of edematous areas to some extent. In addition, the low contrast between the edema region and the adjacent bright blood pool may make the detection of sub-endocardial edema using T_2STIR-bSSFP difficult. A single-shot dark-blood T_2STIR-bSSFP may be a good way to address this issue and will be investigated in our future work. Nevertheless, this study is a proof of concept, designed to demonstrate the feasibility and potential of T_2STIR-bSSFP. It was not a clinical study. Our future work will evaluate the strength, limitations and the optimal threshold value for the segmentation of edema in T_2STIR-bSSFP images, and establish the clinical relevance of T_2STIR-bSSFP in a clinical setting through a large patient cohort.

Conclusion

This study proposes T_2STIR-bSSFP that exploits the elevation of both T_1 and T_2 values of edema to increase the contrast between edematous and normal myocardium. The single-shot technique provides a fast and robust method for myocardial edema imaging with improved contrast compared with several other edema imaging techniques at 3 T.

Supplementary information

Supplementary information accompanies this paper at https://doi.org/10.1186/s12968-019-0583-y.

Additional file 1. 1. The formulas for Signal difference, SNR, CNR and contrast ratio. 2. The extent of edema identified using different methods. 3. The effect of arrhythmia on T_2 maps.

Abbreviations

AFP: Adiabatic full passage; AHP: Adiabatic half passage; AMI: Acute myocardial infarction; bSSFP: Balanced steady state free precession; CMR: Cardiovascular magnetic resonance; CNR: Contrast-to-noise ratio; ECG: Electrocardiogram; IRB: Institutional review board; LFA: Linear flip angle pulses; LGE: Late gadolinium enhancement; mBIR-4: Modified B_1-insensitive rotation pulse; rAHP: Reverse adiabatic half passage; ROI: Region of interest; SAR: Specific absorption rate; SD: Standard derivation; SI: Signal intensity; SNR: Signal-to-noise ratio; SPAIR: Spectral attenuated inversion recovery; STEMI: ST elevation myocardial infarction; STIR: Short tau inversion recovery; T_2p-bSSFP: T_2-prepared balanced steady state free precession; T_2STIR-bSSFP: T_2 prepared inversion with short tau inversion recovery balanced steady state free precession; TSE: Turbo spin echo

Acknowledgements

The authors would like to thank Dr. Raymond Kwong from Brigham and Women's Hospital for his insightful comments on the manuscript.

Authors' contributions

YZ and YCC designed the sequence and experiments and prepared the manuscript. YC and DY performed data collection. LZ performed data analysis. XL edited the manuscript. All authors read and approved the final manuscript.

Funding

This work was supported in part by the National Natural Science Foundation of China (No. 61771463, 81971611, 81830056) and the National Key Research and Development Program of China (No. 2017YFC0112903).

Availability of data and materials

The datasets are available from the corresponding author upon reasonable request.

Ethics approval and consent to participate

The healthy subject study was approved by the institutional review board (IRB) at Shenzhen Institutes of Advanced Technology, and the patient study was approved by the IRB of West China Hospital.

Consent for publication

Written informed consent was obtained from all subjects for publication of their individual details and accompanying images in this manuscript.

Competing interests

Dr. Yiu-Cho Chung is an employee of Siemens Healthcare, Singapore. The other authors declare that they have no competing interests.

Author details

[1]Paul C. Lauterbur Research Centre for Biomedical Imaging, Shenzhen Institutes of Advanced Technology, Guangdong 518055, China. [2]Department of Cardiology, West China Hospital, Chengdu 610041, China. [3]Siemens Healthcare Pte Ltd., 60 MacPherson Road, Singapore 348615, Singapore.

Received: 27 October 2018 Accepted: 22 October 2019
Published online: 21 November 2019

References

1. Eitel I, Friedrich MG. T2-weighted cardiovascular magnetic resonance in acute cardiac disease. J Cardiovasc Magn Reson. 2011;13:13.
2. Friedrich MG. Myocardial edema--a new clinical entity? Nat Rev Cardiol. 2010;7:292–6.
3. Abdel-Aty H. Myocardial edema imaging of the area at risk in acute myocardial infarction seeing through water. JACC Cardiovasc Imaging. 2009; 2:832–4.
4. Simonetti OP, Finn JP, White RD, Laub G, Henry DA. "black blood" T2-weighted inversion-recovery MR imaging of the heart. Radiology. 1996; 199:49–57.
5. Abdel-Aty H, Simonetti O, Friedrich MG. T2-weighted cardiovascular magnetic resonance imaging. J Magn Reson Imaging. 2007;26:452–9.
6. Kim HW, Van Assche L, Jennings RB, Wince WB, Jensen CJ, Rehwald WG, Wendell DC, Bhatti L, Spatz DM, Parker MA, et al. Relationship of T2-weighted MRI myocardial Hyperintensity and the ischemic area-at-risk. Circ Res. 2015;117:254–65.
7. Lauenstein TC, Sharma P, Hughes T, Heberlein K, Tudorascu D, Martin DR. Evaluation of optimized inversion-recovery fat-suppression techniques for T2-weighted abdominal MR imaging. J Magn Reson Imaging. 2008;27:1448–54.
8. Kellman P, Aletras AH, Mancini C, McVeigh ER, Arai AE. T2-prepared SSFP improves diagnostic confidence in edema imaging in acute myocardial infarction compared to turbo spin echo. Magn Reson Med. 2007;57:891–7.
9. Payne AR, Casey M, McClure J, McGeoch R, Murphy A, Woodward R, Saul A, Bi XM, Zuehlsdorff S, Oldroyd KG, et al. Bright-blood T2-weighted MRI has higher diagnostic accuracy than dark-blood short tau inversion recovery MRI for detection of acute myocardial infarction and for assessment of the ischemic area at risk and myocardial salvage. Circ Cardiovasc Imaging. 2011; 4:210–9.
10. Viallon M, Mewton N, Thuny F, Guehring J, O'Donnell T, Stemmer A, Bi X, Rapacchi S, Zuehlsdorff S, Revel D, Croisille P. T2-weighted cardiac MR assessment of the myocardial area-at-risk and salvage area in acute reperfused myocardial infarction: comparison of state-of-the-art dark blood and bright blood T2-weighted sequences. J Magn Reson Imaging. 2012;35: 328–39.
11. Aletras AH, Kellman P, Derbyshire JA, Arai AE. ACUT2E TSE-SSFP: a hybrid method for T2-weighted imaging of edema in the heart. Magn Reson Med. 2008;59:229–35.

12. Giri S, Chung YC, Merchant A, Mihai G, Rajagopalan S, Raman SV, Simonetti OP. T2 quantification for improved detection of myocardial edema. J Cardiovasc Magn Reson. 2009;11:56.
13. Giri S, Shah S, Xue H, Chung YC, Pennell ML, Guehring J, Zuehlsdorff S, Raman SV, Simonetti OP. Myocardial T(2) mapping with respiratory navigator and automatic nonrigid motion correction. Magn Reson Med. 2012;68:1570–8.
14. Baessler B, Schaarschmidt F, Stehning C, Schnackenburg B, Maintz D, Bunck AC. Cardiac T2-mapping using a fast gradient echo spin echo sequence - first in vitro and in vivo experience. J Cardiovasc Magn Reson. 2015;17:67.
15. Basha TA, Bellm S, Roujol S, Kato S, Nezafat R. Free-breathing slice-interleaved myocardial T2 mapping with slice-selective T2 magnetization preparation. Magn Reson Med. 2016;76:555–65.
16. van Heeswijk RB, Feliciano H, Bongard C, Bonanno G, Coppo S, Lauriers N, Locca D, Schwitter J, Stuber M. Free-breathing 3 T magnetic resonance T2-mapping of the heart. JACC Cardiovasc Imaging. 2012;5:1231–9.
17. von Knobelsdorff-Brenkenhoff F, Prothmann M, Dieringer MA, Wassmuth R, Greiser A, Schwenke C, Niendorf T, Schulz-Menger J. Myocardial T1 and T2 mapping at 3 T: reference values, influencing factors and implications. J Cardiovasc Magn Reson. 2013;15:53.
18. Akcakaya M, Basha TA, Weingartner S, Roujol S, Berg S, Nezafat R. Improved quantitative myocardial T2 mapping: impact of the fitting model. Magn Reson Med. 2014.
19. Bano W, Feliciano H, Coristine AJ, Stuber M, van Heeswijk RB. On the accuracy and precision of cardiac magnetic resonance T-2 mapping: a high-resolution radial study using adiabatic T-2 preparation at 3T. Magn Reson Med. 2017;77:159–69.
20. Contrast ratio [https://en.wikipedia.org/wiki/Contrast_ratio].
21. Ugander M, Bagi PS, Oki AJ, Chen B, Hsu LY, Aletras AH, Shah S, Greiser A, Kellman P, Arai AE. Myocardial edema as detected by pre-contrast T1 and T2 CMR delineates area at risk associated with acute myocardial infarction. JACC Cardiovasc Imaging. 2012;5:596–603.
22. Bulluck H, White SK, Rosmini S, Bhuva A, Treibel TA, Fontana M, Abdel-Gadir A, Herrey A, Manisty C, Wan SM, et al. T1 mapping and T2 mapping at 3T for quantifying the area-at-risk in reperfused STEMI patients. J Cardiovasc Magn Reson. 2015;17:73.
23. Kumar A, Beohar N, Arumana JM, Larose E, Li D, Friedrich MG, Dharmakumar R. CMR imaging of edema in myocardial infarction using cine balanced steady-state free precession. JACC Cardiovasc Imaging. 2011;4:1265–73.
24. Nordlund D, Klug G, Heiberg E, Koul S, Larsen TH, Hoffmann P, Metzler B, Erlinge D, Atar D, Aletras AH, et al. Multi-vendor, multicentre comparison of contrast-enhanced SSFP and T2-STIR CMR for determining myocardium at risk in ST-elevation myocardial infarction. Eur Heart J Cardiovasc Imaging. 2016;17:744–53.
25. Zhu Y, Yang D, Chen Y, Liang D, Liu X, Chung Y-C: Myocardial Edema Imaging using Single-shot T2STIR Prepared bSSFP. In Proceedings of the 25th Annual Meeting of ISMRM, ; Honolulu, HI, USA. 2017: p.3253.
26. Rakow-Penner R, Daniel B, Yu H, Sawyer-Glover A, Glover GH. Relaxation times of breast tissue at 1.5T and 3T measured using IDEAL. J Magn Reson Imaging. 2006;23:87–91.
27. Nezafat R, Ouwerkerk R, Derbyshire AJ, Stuber M, McVeigh ER. Spectrally selective B1-insensitive T2 magnetization preparation sequence. Magn Reson Med. 2009;61:1326–35.
28. Jenista ER, Rehwald WG, Chen EL, Kim HW, Klem I, Parker MA, Kim RJ. Motion and flow insensitive adiabatic T2 -preparation module for cardiac MR imaging at 3 tesla. Magn Reson Med. 2013;70:1360–8.
29. Deshpande VS, Chung YC, Zhang Q, Shea SM, Li D. Reduction of transient signal oscillations in true-FISP using a linear flip angle series magnetization preparation. Magn Reson Med. 2003;49:151–7.
30. Kellman P, Wilson JR, Xue H, Ugander M, Arai AE. Extracellular volume fraction mapping in the myocardium, part 1: evaluation of an automated method. J Cardiovasc Magn Reson. 2012;14:63.
31. Kali A, Choi EY, Sharif B, Kim YJ, Bi X, Spottiswoode B, Cokic I, Yang HJ, Tighiouart M, Conte AH, et al. Native T1 mapping by 3-T CMR imaging for characterization of chronic myocardial infarctions. JACC Cardiovasc Imaging. 2015;8:1019–30.
32. Basha TA, Tang MC, Tsao C, Tschabrunn CM, Anter E, Manning WJ, Nezafat R. Improved dark blood late gadolinium enhancement (DB-LGE) imaging using an optimized joint inversion preparation and T2 magnetization preparation. Magn Reson Med. 2018;79:351–60.
33. Kellman P, Xue H, Olivieri LJ, Cross RR, Grant EK, Fontana M, Ugander M, Moon JC, Hansen MS. Dark blood late enhancement imaging. J Cardiovasc Magn Reson. 2016;18:77.
34. Wong EC, Liu TT, Luh WM, Frank LR, Buxton RB. T(1) and T(2) selective method for improved SNR in CSF-attenuated imaging: T(2)-FLAIR. Magn Reson Med. 2001;45:529–32.
35. Liu CY, Wieben O, Brittain JH, Reeder SB. Improved delayed enhanced myocardial imaging with T2-prep inversion recovery magnetization preparation. J Magn Reson Imaging. 2008;28:1280–6.
36. Liu CY, Bley TA, Wieben O, Brittain JH, Reeder SB. Flow-independent T(2)-prepared inversion recovery black-blood MR imaging. J Magn Reson Imaging. 2010;31:248–54.
37. Deshpande VS, Shea SM, Li D. Artifact reduction in true-FISP imaging of the coronary arteries by adjusting imaging frequency. Magn Reson Med. 2003;49:803–9.
38. Thavendiranathan P, Walls M, Giri S, Verhaert D, Rajagopalan S, Moore S, Simonetti OP, Raman SV. Improved detection of myocardial involvement in acute inflammatory cardiomyopathies using T2 mapping. Circ Cardiovasc Imaging. 2012;5:102–10.
39. Kellman P, McVeigh ER. Image reconstruction in SNR units: a general method for SNR measurement. Magn Reson Med. 2005;54:1439–47.
40. Simonetti OP, Kim RJ, Fieno DS, Hillenbrand HB, Wu E, Bundy JM, Finn JP, Judd RM. An improved MR imaging technique for the visualization of myocardial infarction. Radiology. 2001;218:215–23.
41. Ferreira VM, Piechnik SK, Dall'Armellina E, Karamitsos TD, Francis JM, Choudhury RP, Friedrich MG, Robson MD, Neubauer S. Non-contrast T1-mapping detects acute myocardial edema with high diagnostic accuracy: a comparison to T2-weighted cardiovascular magnetic resonance. J Cardiovasc Magn Reson. 2012;14:42.

Publisher's Note